Available online at www.sciencedirect.com
SCIENCE DIRECT®
Biochimica et Biophysica Acta 1617 (2003) 69–79
BIOCHIMICA ET BIOPHYSICA ACTA
BBA
www.bba-direct.com

Conformation and self-assembly of a nystatin nitrobenzoxadiazole derivative in lipid membranes

Liana Silva[a], Ana Coutinho[a,b], Alexander Fedorov[a], Manuel Prieto[a,*]

[a] *Centro de Química-Física Molecular, Complexo Interdisciplinar, Instituto Superior Técnico, Av. Rovisco Pais, P-1049-001 Lisbon, Portugal*
[b] *Departamento de Química e Bioquímica, Bloco C8, Faculdade de Ciências, Universidade de Lisboa, R. Ernesto de Vasconcelos, P-1749-016 Lisbon, Portugal*

Received 21 May 2003; received in revised form 9 September 2003; accepted 11 September 2003

Abstract

Nystatin is a polyene (tetraene) macrolide antibiotic presenting antifungal activity that acts at the cellular membrane level. In the present study, we report the interaction of this antibiotic labelled at its amine group with 7-nitrobenz-2-oxa-1,3-diazole (NBD-Nys) with sterol-free and ergosterol- and cholesterol-containing 1-palmitoyl-2-oleoyl-*sn*-glycero-3-phosphocholine (POPC) large unilamellar vesicles (LUV). The mean tetraene to NBD separating distance determined from fluorescence energy transfer measurements increased from 18 to 25.6 Å upon antibiotic binding to the lipid vesicles, indicating that the monomeric labelled antibiotic adopts a more extended conformation in its lipid-bound state than in aqueous solution. The oligomeric state of membrane-bound NBD-Nys was also studied by resonance energy homotransfer between the NBD fluorophores. The decrease measured in its steady state fluorescence anisotropy upon increasing the surface concentration of the NBD-Nys is shown to be consistent with a random distribution of molecules on the surface of the liposomes. This data contradicts the sharp increase measured for nystatin mean fluorescence lifetime in the presence of 10 mol% ergosterol-containing POPC LUV within the same antibiotic concentration range and which is known to report nystatin oligomerization in the lipid vesicles. Therefore, we conclude that the amine group of nystatin is an essential requisite for the supramolecular organization/pore formation of this antibiotic.

Keywords: Antifungal; Polyene macrolide antibiotic; Fluorescence; Nystatin; Energy migration

1. Introduction

Nystatin (Nys) and amphotericin B (AmB) are antifungal antibiotics that permeabilize a wide spectrum of eukaryotic cells, including fungal and mammalian cells, and synthetic lipid vesicles [1]. Membrane sterols are believed to play a role in the antibiotic's activity and it has been proposed that the selective toxicity of these polyene antibiotics for fungi results from their capacity to bind more strongly to ergosterol, the main fungal sterol, than to cholesterol, the main sterol present in mammalian cells [1]. Prevailing models for the mechanism of action of Nys and AmB postulate the formation of transmembrane channels with size-discriminating properties in the plasma membrane of the antibiotic-sensitive organisms [2]. Recently, Gruszecki et al. [3] detected the formation in monolayers of cylindrical structures of AmB with an internal diameter close to 0.6 nm by scanning force microscopy. However, there is no consensus on the pathway of induction of membrane damage by these antibiotics or on the role played by sterols in this process [4]. Several authors have proposed a sequence of three events: binding of the antibiotic monomer to the membrane surface, self-assembly to a prepore oligomer, and insertion in the lipid bilayer generating a functional pore that mediates passive flux of molecules across the membrane [5–7]. Cohen [7,8] further suggested that the initially formed nonaqueous channels subsequently interacted with the sterols in the membrane to form aqueous channels, having an enlarged diameter. Alternatively, Bolard et al. [9] proposed that soluble monomeric AmB is very active towards ergosterol-containing membranes, where classic barrel-stave-type com-

Abbreviations: AmB, amphotericin B; LUV, large unillamelar vesicles; NBD-Nys, (6-[*N*-(4-nitro-2,1,3-benzoxadiazolyl)-aminohexanoyl]nystatin; Nys, nystatin; P10C, 10 mol% cholesterol-containing POPC LUV; P10E, 10 mol% ergosterol-containing POPC LUV; POPC, 1-palmitoyl-2-oleoyl-1-*sn*-glicero-3-phosphocholine

* Corresponding author. Tel.: +351-21-8419219; fax: +351-21-8464455.
E-mail address: prieto@alfa.ist.utl.pt (M. Prieto).

0005-2736/$ - see front matter © 2003 Elsevier B.V. All rights reserved.
doi:10.1016/j.bbamem.2003.09.004

plexes with this sterol are formed, but a soluble self-associated and sterol-free oligomer is required for the permeabilization of cholesterol-containing membranes. On the other hand, other studies have demonstrated the ability of AmB to form channels in sterol-free membranes under specific conditions like when using high antibiotic concentrations [10] and in osmotically stressed liposomes [11,12].

Previous studies from our laboratory have shown that Nys mean fluorescence lifetime is a reporter parameter of its aggregation state in gel-phase DPPC small unilamellar vesicles (SUV) and large unilamellar vesicles (LUV) [13,14] and in ergosterol-containing 1-palmitoyl-2-oleoyl-*sn*-glycero-3-phosphocholine (POPC) LUV [15]. Surprisingly, the fluorescence emission decay kinetics of Nys was found to remain essentially invariant in the presence of cholesterol-containing liposomes [15], although independent data from activity assays suggested that aqueous channels were also formed in these lipid vesicles (Coutinho and Prieto, unpublished work). We proposed that Nys channel architecture must be sterol-dependent, its structure being looser and less stable in cholesterol-containing lipid membranes than in ergosterol-containing lipid membranes. This hypothesis stems from the observation that, in the first case, channel formation was not concurrent with any alterations in Nys fluorescence properties, at variance that was found with ergosterol-containing POPC LUV.

To further explore the proposition that Nys oligomers are formed both in ergosterol- and cholesterol containing POPC LUV, we intended to examine the oligomerization state of Nys in lipid vesicles by carrying out fluorescence homotransfer (donor-to-donor energy transfer or energy migration) measurements. Although Nys is an intrinsically fluorescent antibiotic, its tetraene fluorophore is not suitable for this type of studies due to its large Stokes shift [13]. Therefore, a nitrobenzoxadiazole derivative of Nys (6-[*N*-(4-nitro-2,1,3-benzoxadiazolyl)-aminohexanoyl]nystatin, NBD-Nys), was prepared according to Petersen [16] to carry out an energy migration study among the NBD chromophores on the labelled antibiotic. We have already investigated the conformational flexibility of this labelled antibiotic in different solvents by carrying out fluorescence resonance energy transfer (FRET) measurements between the intrinsic chromophore of Nys (tetraene group) and the NBD label (hetero-FRET measurements) [17]. Here we describe the use of steady state and time-resolved fluorescence spectroscopy to characterize the interaction of NBD-Nys with LUV prepared with a variable lipid composition (0 and 10 mol% cholesterol- or ergosterol-containing POPC LUV). To study the aggregation behaviour of lipid-bound NBD-Nys, the decrease presented by its steady state fluorescence anisotropy upon increasing its surface concentration in the membranes was compared with the theoretical expectation from the two-dimensional homotransfer formalism of Snyder and Freire [18], as well as to another model assuming molecular dimerization [19]. The data could be rationalized assuming a random antibiotic distribution in POPC and 10 mol% cholesterol- or ergosterol-containing POPC LUV, suggesting that chemical modification of Nys amine group influenced its ability to assemble in the lipid vesicles.

2. Materials and methods

2.1. Materials

The polyene antibiotic Nys was obtained form Sigma (St. Louis, MO) and the NBD-hexanoyl derivative of Nys was synthesized and purified as previously described [17]. POPC was purchased from Avanti Polar Lipids (Birmingham, AL), cholesterol was from Sigma, and ergosterol was from Fluka Chemika (Buchs, CH). Stock solutions of cholesterol ($\sim$ 0.1 M) and ergosterol ($\sim$ 0.05 M) were prepared in chloroform and stored at -20 °C with exclusion of light.

2.2. Preparation of liposomes

LUV with a mean diameter of 100 nm were prepared by the extrusion method [20]. Briefly, adequate volumes of POPC and sterol stock solutions in chloroform were mixed at the desired molar ratios (0 and 10 mol% of cholesterol- or ergosterol-containing LUV (P10C or P10E, respectively)) and dried until complete evaporation of the solvent (first under a stream of N_2 and then under vacuum). The residual lipid film, warmed to 50 °C in a water bath, was hydrated with HEPES buffer (20 mM HEPES–NaOH (pH 7.4) with 150 mM NaCl and 1 mM EDTA) and repeatedly vortexed until all lipid was removed from the walls of the round-bottom flask. Then, a freeze–thaw cycle was repeated eight times using liquid nitrogen and a water bath warmed to 50 °C. Subsequently, the lipid suspension was extruded 4 and 10 times through polycarbonate membranes of 400 and 100 nm pore sizes (Nuclepore, Pleasanton CA, USA), respectively. This stock solution was stored at 4 °C. The final phospholipid concentration was determined by phosphate analysis [21].

2.3. NBD-nystatin partitioning experiments

The dependence of NBD-Nys partition coefficient on the lipid composition of the liposomes used was assessed from the increase in the fluorescence intensity of the NBD fluorophore upon its partitioning into the lipid bilayers. To rule out the possible interference of photobleaching effects, two different methodologies were used, which were found to give essentially equivalent results. In the first case, several dilutions of a LUV stock solution (ca. 7 mM) were prepared with HEPES buffer and 2 μl of an NBD-Nys stock solution in methanol was injected to each of these samples (final antibiotic concentration 2.5 μM). After an incubation time of 1 h in the dark and at room temperature, the fluorescence signal of each sample was monitored as a function of the

lipid concentration used (λ_{ex} = 467 nm, λ_{em} = 535 nm). The contribution of the liposomes alone was subtracted from this intensity. In the second method, an aqueous solution of NBD-Nys was progressively titrated with a concentrated suspension of LUV (ca. 15 mM). The samples were magnetically stirred continuously in 1 × 1 cm quartz cuvettes. Fifteen minutes after each liposome addition, the fluorescence intensity of the sample was measured in the conditions indicated above. All fluorescence intensities were subtracted of the signal of an analogous vesicle preparation containing no antibiotic and corrected for the progressive dilution of the sample. The incorporation kinetics of NBD-Nys into the lipid vesicles was independently controlled and shown to be essentially complete 7 min after the antibiotic addition to the lipid suspension.

The experimental data were analyzed according to Eq. (1) [22]:

$$\Delta I = \frac{\Delta I_{max} K_p [L]_{ac}}{[W] + K_p [L]_{ac}} \quad (1)$$

In this equation, $\Delta I = I - I_0$ stands for the difference between the steady state fluorescence intensity of the antibiotic measured in the presence (I) and in the absence (I_0) of phospholipid vesicles; $\Delta I_{max} = I_\infty - I_0$ is the maximum value of this difference, because I_∞ is the limiting value of I measured upon increasing the lipid concentration, [L], of the solution; K_p is the mole-fraction partition coefficient of the antibiotic between the aqueous and lipid phases and [W] is the molar concentration of water. It was assumed that only 50% of the overall lipid used was accessible, $[L]_{ac}$, for the initial partitioning of the antibiotic.

The partition coefficient of the antibiotic can be used to compute the mole fraction of membrane-bound monomeric antibiotic molecules, x_m, at different lipid concentrations:

$$x_m = \frac{K_p [L]_{ac}}{[W] + K_p [L]_{ac}} \quad (2)$$

2.4. Absorption and steady state fluorescence measurements

Absorption spectroscopy was carried out with a Jasco V-530 or V-560 spectrophotometer. When necessary, absorption spectra were corrected for turbidity by subtracting an appropriate blank sample.

Steady state fluorescence measurements were carried out with an SLM-Aminco 8100 Series 2 spectrofluorimeter in a right angle geometry as described [17]. Emission spectra were collected for Nys and the NBD-labelled antibiotic, with λ_{ex} at 319 and 467 nm, respectively, whereas excitation spectra were collected with λ_{em} at 410 and 535 nm for the tetraene and NBD chromophores, respectively. The slit widths for the excitation and emission monochromators were 4 nm. Fluorescence quantum yields for the tetraene and NBD chromophores of Nys and NBD-Nys were determined using as references quinine bisulfate in 0.1 N sulfuric acid (Φ_R = 0.52) [23] and coumarin 6 in ethanol (Φ_R = 0.78) [24], respectively.

For fluorescence anisotropy measurements, Glan-Thompson polarizers were used. Steady state fluorescence anisotropies, $\langle r \rangle$, were calculated from [25]:

$$\langle r \rangle = \frac{I_{VV} - G I_{VH}}{I_{VV} + 2 G I_{VH}} \quad (3)$$

where the different intensities I_{ij} are the steady state vertical and horizontal components of the fluorescence emission with excitation vertical (I_{VV} and I_{VH}) and horizontal (I_{HV} and I_{HH}) to the emission axis. The later pair of components is used to calculate the G factor ($G = I_{HV}/I_{HH}$). An adequate blank was subtracted from each intensity reading before the calculation of the anisotropy value.

Considering that the anisotropy is additive, we have:

$$\langle r \rangle = \sum f_i \langle r \rangle_i \quad (4)$$

where $\langle r \rangle_i$ is the steady state fluorescence anisotropy of each species (i = w or i = m for the lipid-free and membrane-bound antibiotic species, respectively). The fractional contribution to the steady state fluorescence of component i is given by:

$$f_i = x_i \varepsilon_i g_i \Phi_i / \Sigma x_i \varepsilon_i \Phi_i g_i \quad (5)$$

where x_i, ε_i, Φ_i, and g_i are the fractional population, the molar absorption coefficient, the fluorescence quantum yield, and the fluorescence intensity at the emission wavelength in a normalized spectrum of each species, respectively.

2.5. Time-resolved fluorescence measurements

Fluorescence decay measurements were carried out with a time-correlated single-photon timing system, which is described elsewhere [26]. Excitation and emission wavelengths were 319 and 410 nm for the tetraene chromophore, respectively, and 467 and 535 nm for the NBD chromophore, respectively. Time scales were chosen for each sample in order to observe the decay through 2–3 intensity decades. Experimental response functions for deconvolution were generated from a scattering dispersion (silica, colloidal water suspension, Aldrich, Milwaukee, WI). Data analysis was carried out using a nonlinear squares iterative convolution method based on the Marquardt algorithm. The decays were analyzed empirically by fitting a sum of exponentials (Eq. (6))

$$I(t) = \sum_{i=1}^{n} \alpha_i \exp(-t/\tau_i) \quad (6)$$

where α_i and τ_i are the normalized amplitude and lifetime of component i, respectively. The goodness of the fits was judged from the experimental χ^2 values, weighted residuals,

and autocorrelation plots. The lifetime-weighted quantum yield is given by:

$$\bar{\tau} = \Sigma \alpha_i \tau_i \tag{7}$$

2.6. Data analysis

In this study, the extent of fluorescence radiationless energy transfer, E, was measured by both steady state and time-resolved fluorescence methodologies using separate donor-only (D = Nys) and donor/acceptor (DA = NBD-Nys) samples. The energy transfer efficiency based on the decrease in the fluorescence intensity of the donor was calculated using:

$$E = 1 - \frac{I_{DA}}{I_D} \tag{8}$$

where I_D and I_{DA} are the steady state fluorescence intensities of the donor in the absence and in presence of the acceptor, respectively. This efficiency can also be calculated from the donor lifetime-weighted quantum yields obtained in the absence, $\bar{\tau}_D$, and in the presence of the acceptor, $\bar{\tau}_{DA}$, as in Eq. (9):

$$E = 1 - \frac{\bar{\tau}_{DA}}{\bar{\tau}_D} \tag{9}$$

Whenever it was necessary, data were corrected for eventual artefacts present in a steady state experimental approach to energy transfer measurements in a right-angle geometry as previously described [27].

The interfluorophore distance, R, is calculated from the efficiency using:

$$R = R_o \left(\frac{1}{E} - 1 \right)^{1/6} \tag{10}$$

where R_o is the Förster radius for the donor and acceptor pair. This distance is characteristic of a specific transfer pair and situation, and is proportional to the sixth root of the overlap integral, J:

$$R_o = 0.2108 [\kappa^2 \Phi_F n^{-4} J]^{1/6} \tag{11}$$

This integral describes the resonance between the donor and the acceptor dipoles and was evaluated by integration of the mutual area of overlap between the normalized donor emission spectrum, $I(\lambda)$, and the acceptor absorption spectrum, $\varepsilon(\lambda)$ (in M^{-1} cm^{-1} units), as defined by:

$$J = \int_0^\infty I(\lambda)\varepsilon(\lambda)\lambda^4 d\lambda \tag{12}$$

In Eq. (11), R_o is expressed in Å units, κ^2 is the orientational factor, Φ_F is the quantum yield of the donor probe in the absence of acceptor, n is the refractive index of the medium, and the wavelength is expressed in nm units. For the orientational factor, we make the usual assumption $\kappa^2 = 2/3$, i.e., dynamic isotropic regime of energy transfer [28].

3. Results

3.1. NBD-nystatin binding to the lipid vesicles

The influence of NBD-Nys binding to the lipid vesicles on its fluorescence emission properties is illustrated in Fig. 1B for P10C LUV. There was a 15 nm blueshift in NBD-Nys fluorescence emission maximum from 562 nm in HEPES buffer to 547 nm in the presence of 6 mM P10C LUV, coupled to an increase in fluorescence intensity (see below). These spectroscopic changes suggest a superficial localization for the NBD fluorophore in the labelled Nys, near the head group region of the lipid bilayer [29,30]. The light scattering intensity at 90° ($\lambda_{ex} = \lambda_{em} = 550$ nm) of NBD-Nys-treated LUV was also monitored. This parameter was not affected by the addition of the labelled-antibiotic (0–25 μM) to the lipid vesicles,

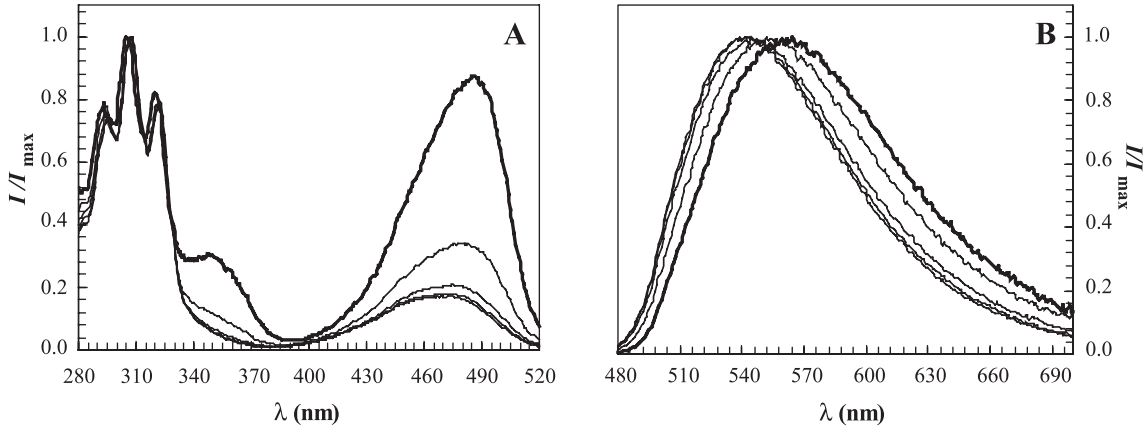

Fig. 1. Normalized (A) excitation ($\lambda_{em} = 535$ nm) and (B) emission ($\lambda_{ex} = 467$ nm) spectra of NBD-Nys in the presence of 0, 0.5, 2, 4, and 6 mM P10C LUV (A: from top to bottom and B: from right to left, respectively). The spectra obtained in HEPES buffer are presented in bold.

indicating that neither aggregation nor fusion of the liposomes occurred, independently of its lipid composition (data not shown). Similar data were obtained with POPC and P10E LUV.

The increase in NBD fluorescence intensity was used to monitor the interaction of NBD-Nys with lipid vesicles. All the experimentally determined partitioning curves presented the expected hyperbolic behaviour (data not shown), and the partition coefficients recovered from the fit of Eq. (1) to these data, are presented in Table 1. The lipid composition of the vesicles had a minimal influence on NBD-Nys binding to the liposomes, the antibiotic derivative always presenting a relatively low partition coefficient ($K_p \approx 1.3 \times 10^4$ for POPC, P10C, and P10E LUV (Table 1). These partition coefficients were slightly smaller than the ones obtained for the parent compound Nys in the same conditions (K_p(Nys/POPC) = 1.7×10^4; K_p(Nys/P10C) = 1.8×10^4; K_p(Nys/P10E) = 1.4×10^4) (data not shown). This result shows that the labelling of Nys with NBD slightly decreased the affinity of the antibiotic for the lipid vesicles, probably due to the high polarity of this fluorophore. These variations in K_p, however, had a minimal effect upon the membrane-bound antibiotic fractions computed from Eq. (2), which changed from approximately 25% to 30% for NBD-Nys and Nys, respectively, in the experimental conditions used in this work (total lipid concentration of 3 mM).

Membrane binding of NBD-Nys was also examined on the basis of changes undergone by the steady state fluorescence anisotropy of the NBD fluorophore upon its partition to the lipid vesicles. As it is exemplified in Fig. 2 for POPC LUV, the fluorescence anisotropy of the NBD fluorophore progressively increased from $\langle r \rangle \approx 0.055$ in aqueous solution towards a plateau value of $\langle r \rangle \approx 0.145$ in 6 mM POPC LUV, which is consistent with a more restricted rotational freedom experienced by the NBD label upon membrane binding. These measurements are already corrected for the expected decrease in the anisotropy values caused by an increased turbidity of the sample due to the addition of lipid vesicles (the highest correction performed was less than 10% for 6 mM POPC LUV). It should also be noted that energy homotransfer (see below) is not biasing these measurements because a very low antibiotic concentration was used in this experiment. The fluorescence anisotropy data

Table 1
Mole fraction partition coefficients, K_p, and steady state fluorescence quantum yields, $\Phi_m^{NBD\text{-}Nys}$ (NBD chromophore), of NBD-Nys in interaction with POPC LUV with a variable sterol content (P10C and P10E: 10 mol% cholesterol- and ergosterol-containing POPC LUV, respectively)

Sample	K_p ($\times 10^4$)	$\Phi_m^{NBD\text{-}Nys}$	J ($\pm 0.2 \times 10^{14}$ M^{-1} cm^{-1} nm^4)	R_o (± 1.2 Å)
POPC	(1.2 ± 0.1)	0.47	1.2	31.0
P10C	(1.4 ± 0.2)	0.35	1.5	30.4
P10E	(1.3 ± 0.9)	0.28	1.3	28.8

The overlap integrals, J, and Förster radius, R_o, are calculated for the NBD–NBD pair.

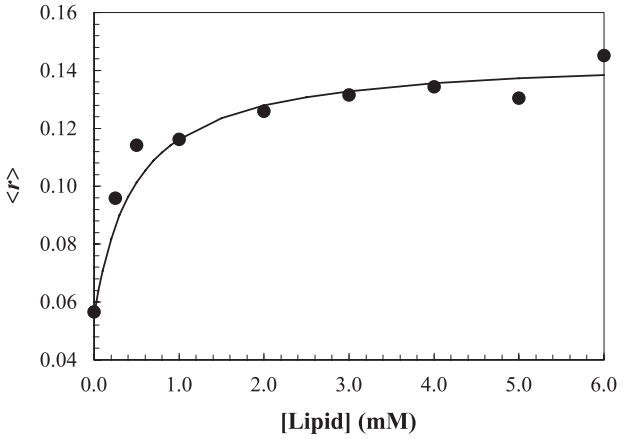

Fig. 2. Steady state fluorescence anisotropies of 2.5 μM NBD-Nys in the presence of POPC LUV (λ_{ex} = 467 nm, λ_{em} = 535 nm). The fluorescence anisotropy data could be well described by Eq. (4) (solid line) assuming $\varepsilon_w = \varepsilon_m$, $\Phi_w^{NBD\text{-}Nys} = 0.03$ and $\langle r \rangle_m = 0.145$. It was further considered $g_w = 0.8$ and $g_m = 1.0$, $\langle r \rangle_w = 0.055$ and $\Phi_m^{NBD\text{-}Nys}$ (POPC LUV) = 0.47, which was calculated using $K_p = 1.2 \times 10^4$. See text for details.

could be well described by Eq. (4) assuming $\varepsilon_w = \varepsilon_m$, $\Phi_w^{NBD} = 0.03$ [24] and $\langle r \rangle_m = 0.145$. The following values, which were determined experimentally, were also used in the fitting: $g_w = 0.8$ and $g_m = 1.0$, $\langle r \rangle_w = 0.055$, and Φ_m^{NBD} (POPC LUV) = 0.47 that was calculated using $K_p = 1.2 \times 10^4$ (Table 1). These data shows that although, e.g., for 3 mM POPC LUV only about 25% of NBD-Nys is membrane-bound, its fluorescence anisotropy has practically reached its limiting value in the membrane, because the quantum yield of the NBD label increases 16-fold upon membrane binding. This result is the basis for selecting 3 mM for the lipid concentration to be used in the homotransfer studies (see below).

The fluorescence decays of the NBD probe conjugated to the antibiotic in the presence of 3 mM liposomes were complex, requiring a two- or three-exponential law for good fits to be obtained (Table 2: λ_{em} = 535 nm). As it was explained above, these decays were largely dominated by the fluorescence emitted by the membrane-bound molecules (their fractional contribution to the steady state intensity was around 66–84% in the experimental conditions used (Eq. (2) and Table 1). In the presence of P10E LUV, a suitable fit was obtained using two decay times of 1.2 and 6.9 ns (fractional intensities of approximately 20% and 80%, respectively (Table 2)). However, in the presence of POPC or P10C LUV, an additional longer decay time of about 8.6–9.9 ns (fractional intensities of 36% and 45%, respectively) was required to improve the quality of the fits (Table 2). This implies a more heterogeneous environment for the NBD probe in these two lipid membranes [29]. For each lipid composition studied, the lifetime-weighted quantum yield of the NBD probe in NBD-Nys was independent of the antibiotic concentration in each sample (Table 2), showing that this fluorophore was not dynamically self-quenched.

Table 2
Normalized fluorescence amplitudes, α_i, and lifetimes, τ_i, of nystatin, Nys, and of its labelled analogue, NBD-Nys, in interaction with 3 mM POPC LUV prepared with a variable sterol content (P10C and P10E: 10 mol% cholesterol-and ergosterol-containing POPC LUV, respectively) (λ_{ex} = 319 nm)

Lipid	Sample	λ_{em} (nm)	c (μM)	n	α_1	τ_1 (ns)	α_2	τ_2 (ns)	α_3	τ_3 (ns)	α_4	τ_4 (ns)	$\bar{\tau}$ (ns)	χ^2
POPC	NBD-Nys	535	2.5–25	6	0.43	1.16	0.33	5.96	0.24	8.55			4.54	1.0–1.3
P10C	Nys	410	2.5–25	6	0.34	0.17	0.24	1.07	0.29	3.72	0.12	8.60	2.43	1.0–1.3
	NBD-Nys	410	2.5–25	6	0.61	0.05	0.26	0.20	0.09	1.10	0.04	5.70	0.41	1.0–1.2
		535	2.5–25	7	0.45	1.13	0.38	6.45	0.17	9.85			4.60	1.0–1.3
P10E	Nys	410	7.5		0.74	1.09	0.12	6.35	0.14	46.4			8.17	1.1
			10.0		0.70	1.00	0.12	5.66	0.18	45.1			9.37	1.1
			12.5		0.65	1.11	0.13	6.69	0.21	46.6			11.6	1.1
			15.0		0.60	1.18	0.14	7.53	0.26	47.1			13.9	1.1
			25.0		0.47	1.26	0.16	7.75	0.37	46.8			19.0	1.2
	NBD-Nys	410	7.5		0.23	0.22	0.72	0.94	0.06	3.04			0.89	1.1
			10.0		0.26	0.17	0.67	0.89	0.07	2.88			0.85	1.1
			12.5		0.29	0.15	0.63	0.87	0.08	2.79			0.81	1.2
			15.0		0.34	0.13	0.58	0.85	0.08	2.75			0.75	1.2
			25.0		0.42	0.11	0.49	0.79	0.09	2.65			0.67	1.3
		535	2.5–25	7	0.58	1.17	0.42	6.93					3.61	1.0–1.3

c is the antibiotic concentration used and $\bar{\tau}$ is calculated as $\bar{\tau} = \Sigma \alpha_i \tau_i$. Some results are the mean of n independent experiments.

3.2. Hetero-FRET measurements in the membrane

To evaluate if the transfer of NBD-Nys from the aqueous phase to the lipid membrane had any influence upon the conformation adopted by the labelled antibiotic, we carried out hetero-FRET measurements between the tetraene and NBD fluorophores in the presence of liposomes. The lipid composition of the vesicles employed in these studies was chosen to be P10C LUV due to the fact that the fluorescence emission decay kinetics of Nys is not concentration-dependent (Table 2) in the presence of this type of lipid vesicles, which simplifies data analysis (see below).

Upon increasing the lipid concentration in solution, the vibrational progression typical of a tetraene band gradually dominated the excitation spectra of NBD-Nys in the 250–350 nm region (λ_{em} = 535 nm) (Fig. 1A). This result indicates that the transfer efficiency from the tetraene to the NBD chromophore in NBD-Nys is much higher in the membrane-bound molecules than in aqueous solution (it should be noted that Nys does not emit at 535 nm). Because quantum yield and spectral shape are also environment sensitive, Förster distances vary as solution condition does, which could be a possible explanation for the data obtained [17]. This hypothesis was confirmed through the calculation of R_o(tetraene/NBD pair) in aqueous solution and in the presence of P10C LUV. If we use 0.001 for the quantum yield of Nys in aqueous solution [31], $J = 3.7 \times 10^{14}$ M^{-1} cm^{-1} nm^4 (the same value as the one obtained for the Nys and NBD-hexanoate pair in methanol [17]), n = 1.33 and $\kappa^2 = 2/3$, we get R_o = 13.8 Å using Eq. (11). The Förster radius for the tetraene/NBD pair increased to 33.5 Å in the presence of the lipid vesicles, a change that was mainly due to the higher quantum yield measured for the lipid-bound tetraene donor group in Nys ($\Phi_m^{Nys} = 0.25$) relatively to its value in aqueous solution. In this calculation, the experimentally determined overlap integral for the membrane-bound donor–acceptor pair $J = 3.7 \times 10^{14}$ M^{-1} cm^{-1} nm^4 was used, as well as n = 1.4 (the interface location of the antibiotic justifies this assumption), and $\kappa^2 = 2/3$.

The fluorescence emission decay kinetics of Nys was independent of the antibiotic concentration used in the presence of 3 mM P10C LUV (Table 2, λ_{em} = 410 nm), as previously reported [15]. The multiexponential analyses for Nys and NBD-Nys fluorescence decays obtained in the presence of these liposomes showed a shortening of the lifetime-weighted quantum yield of the tetraene donor by the presence of the acceptor chromophore NBD in the labelled antibiotic (Table 2), evidencing the occurrence of an efficient intramolecular energy transfer process between the tetraene/NBD pair. Using Eqs. (8) and (9), the energy transfer efficiencies in NBD-Nys in the presence of 3 mM P10C LUV based on the decrease in the fluorescence intensity and lifetime-weighted quantum yield of the donor were found to be (93 ± 3)% and (83 ± 5)% (n = 6), respectively. The comparison between the steady state and time-resolved efficiencies show that some static quenching occurs in NBD-Nys, as previously described for homogeneous solution [17]. As it is shown in Appendix A, the measured overall energy transfer efficiencies can be assumed to be equal to the values presented by the membrane-bound antibiotic molecules, i.e., they are not affected by the fraction of the antibiotic in the aqueous phase because (i) the partition coefficients of Nys and NBD-Nys are very similar and; (ii) $\Phi_m^{Nys} \approx 250\Phi_w^{Nys}$. After introducing these values in Eq. (10), a mean tetraene-to-NBD distances of (21.7 ± 1.5) Å and (25.7 ± 0.6) Å are recovered for the membrane-bound labelled antibiotic from the steady state and time-resolved fluorescence measurements, respectively. The steady state data gives a biased shorter distance due to the small static (eventually exchange mechanism) quenching contribution. This result was independent of the concentrations of Nys and NBD-Nys used in these experiments (2.5–25 μM).

Previously, we have determined that for NBD-Nys in methanol, the mean apparent interfluorophore distances recovered from steady state and time-resolved fluorescence measurements were (15.2 ± 1.5) Å and (17.7 ± 0.6) Å, respectively [17]. Assuming that the conformational equilibrium of NBD-Nys in aqueous solution is identical to its behaviour in methanol, there is an almost 8 Å increase in the average separation between the NBD- and polyene-chromophores in NBD-Nys upon its partition into the lipid vesicles. Therefore, we conclude that NBD-Nys adopts preferentially a more extended conformation upon binding to the cholesterol-containing LUV. This conformation is probably stabilized by the anchoring of its NBD group at the membrane interface, in agreement with the NBD spectroscopic data presented above.

The time-resolved fluorescence studies carried out with Nys in the presence of the ergosterol-rich lipid vesicles clearly evidenced the formation of long-lived antibiotic species upon increasing the antibiotic concentration in solution (Table 2, λ_{em} = 410 nm), an effect that is known to accompany Nys oligomerization in the lipid vesicles [13–15]. The putative aggregation of the antibiotic raises two potential problems in the analysis of the hetero-FRET measurements carried out for NBD-Nys in these liposomes. First, Nys molecules participating in aggregate formation must have a higher fluorescence quantum yield, and, therefore, a higher R_o. Second, the transfer efficiency is expected to increase in a cluster of NBD-Nys molecules due to the presence of more than one nearby potential NBD acceptor for each tetraene chromophore (donor). In the absence of additional information about the fraction of membrane-bound antibiotic molecules involved in aggregate formation and about their stoichiometry and geometry, we will not attempt to rationalize these data.

3.3. Fluorescence self-quenching and homo-FRET measurements between lipid-bound NBD-Nys

Self-quenching of NBD fluorescence is a known photophysical process [32] that can be used to report the eventual NBD-Nys aggregation in the membrane. As it was mentioned before, NBD fluorescence lifetime was found to be concentration-independent (Table 2, λ_{em} = 535 nm), ruling out the occurrence of a dynamic self-quenching mechanism between the membrane-bound NBD-Nys molecules. The antibiotic derivative participating in oligomer formation could also undergo a static fluorescence quenching process. This hypothesis (formation of nonfluorescent or "dark" oligomers) was also discarded because a linear variation of NBD steady state fluorescence intensity vs. antibiotic concentration was obtained (results not shown). However, NBD-Nys aggregation in the lipid vesicles cannot be completely excluded from these data because fluorescent antibiotic oligomers may be formed by NBD-Nys if the NBD-fluorophores are kept in a nonmolecular contact situation.

The small Stokes shift exhibited by the NBD fluorophore raises the possibility of using homo-FRET measurements between NBD chromophores to further investigate the formation of these species in the membrane [33,34]. From the spectral properties of the lipid-bound NBD probe, a Förster radius of (30.1 ± 1.1) Å was calculated for the NBD/NBD pair in the presence of POPC LUV prepared with variable sterol content (Table 2). Energy migration between NBD chromophores was determined using steady state fluorescence anisotropy measurements, and it was found that an increase in the concentration of fluorophores on the membrane surface resulted in a slight depolarization of its fluorescence (Fig. 3A). In the present case, the important question is whether the concentration-dependent depolariza-

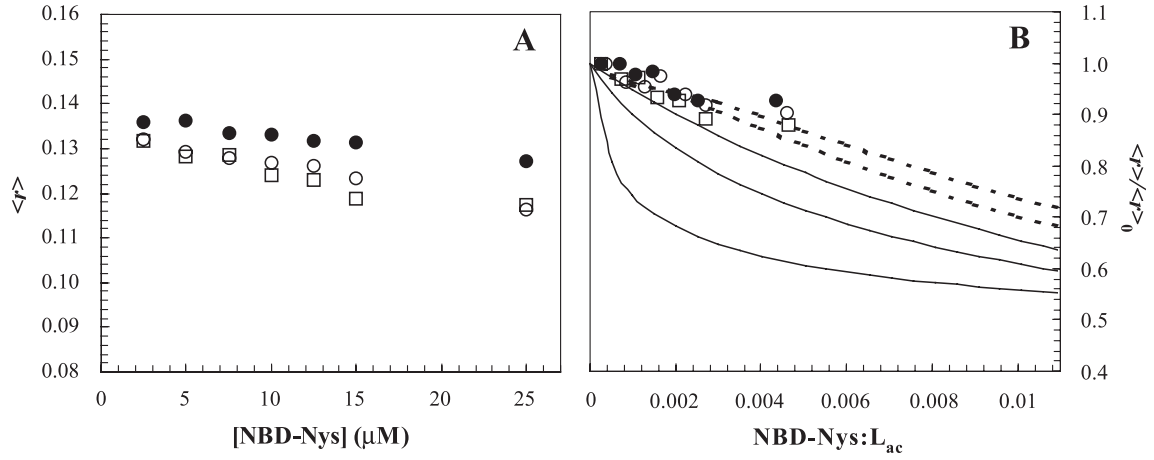

Fig. 3. (A) Steady state fluorescence anisotropies of NBD-Nys in the presence of 3 mM POPC (filled circles), P10C (open circles), and P10E (open squares) LUV (λ_{ex} = 467 nm, λ_{em} = 535 nm). (B) Normalized anisotropy (to infinite dilution ([NBD-Nys] = 2.5 μM)) of NBD-Nys as a function of its surface concentration in the lipid vesicles. The dotted lines are Monte Carlo simulations according to the formalism of Snyder and Freire [18] using different distances of closest approach between the molecules, L. From top to bottom: L = 15 Å and L = 7.5 Å. The solid lines are simulations for the anisotropy in a monomer/dimer system according to Loura and Prieto [19] using different dissociation constants, K_d. From top to bottom, K_d = 0.05, 0.01, and 0.001 mol/mol lipid, implying a progressive increase in the dimer fraction present in the lipid vesicles. See text for details.

tion undergone by NBD-Nys is only the consequence of a random distribution of NBD-antibiotic molecules in the membrane surface or the result of high local surface densities of the antibiotic due to its self-association. To discriminate between these two hypotheses, the formalism of Snyder and Freire [18] was used to predict the depolarization dependence for a random distribution of fluorophores on a bilayer surface. These authors used Monte Carlo simulations to describe depolarization by energy migration in a planar surface assuming an isotropic distribution of fluorophore absorption and emission dipoles and a distance L of closest approach between molecules, which appears as a parameter in their model. The theoretical homotransfer curves obtained according to Snyder and Freire [18] are represented in Fig. 3B for $L=7.5$ Å and $L=15$ Å (dotted lines). These L values were chosen because the lateral dimensions of a monomeric antibiotic molecule (see below) are within this range. Average surface areas per lipid molecule (63 and 58 Å^2 for POPC and P10C/P10E LUV, respectively), which are necessary for computing the surface concentrations, were taken from Smaby et al. [35]. In these plots, the anisotropy values are normalized to the value obtained in dilute solutions, $\langle r\rangle_o$ (in our case we used the sample with 2.5 μM NBD-Nys). In addition, theoretical curves describing the expected behaviour for the anisotropy in a monomer/dimer system calculated according to the model of Loura and Prieto [19] are also plotted in Fig. 3B (solid lines) assuming different dimerization constants for the labelled-antibiotic. In these simulations, it was assumed that there is energy transfer among monomers and from monomers to dimers. In addition, it is considered that each directly excited dimer could be treated as an isolated pair of molecules (the distance between them being fixed and assumed to be equal to 15 Å), because the probability of transfer to a third molecule is much smaller than that of decay (either radiative or nonradiative) or transfer to the other molecule involved in the dimer. Using Eq. (A12) in Ref. [19], we computed that the anisotropy of the putative dimers formed in the membrane was 0.076. From Fig. 3B, it is clear that in all the lipid vesicles studied (POPC, P10C, and P10E LUV), there is a good qualitative agreement between the theoretical concentration-dependent depolarization curves calculated assuming a random surface distribution of fluorophores and the experimental data.

4. Discussion

In the present work, we planned to examine Nys oligomerization in lipid bilayers using a homo-FRET (energy migration) methodology. The NBD chromophore has a small Stokes shift, thereby presenting a significant R_o value, allowing for energy migration studies to be carried out. Furthermore, since the absorption and fluorescence properties of the NBD chromophore are environmentally sensitive and change dramatically upon varying the bulk polarity of the medium [24,36], spectroscopic partition studies were also carried out, allowing to quantify the interaction established between NBD-Nys and the lipid vesicles.

4.1. Solution and membrane-bound conformations of the polyene antibiotic nystatin

In the first part of this study, we extended the earlier intramolecular hetero-FRET study carried out with NBD-Nys in homogeneous solution [17] to the lipid vesicles in order to evaluate if the transfer of the labelled-antibiotic from the aqueous medium to the lipid membrane was associated with a conformational change. In fact, given the likely importance of the solution vs. membrane structure in the activity of this class of antibiotics, the elucidation of their structure in both environments is an important issue. Our time-resolved data shows that the mean tetraene-to-NBD distance increased almost 8 Å upon its binding to P10C LUV, reporting a partial unfolding of the monomeric labelled-antibiotic towards a more extended conformation in its membrane-bound state (Fig. 4A and B). This shift in the conformational equilibrium of NBD-Nys may be attributed to the interactions established between the membrane and the NBD label, which must stabilize the more open conformer at the lipid–water interface. Although NBD is an aromatic molecule, it carries localized charges as well a dipole moment arising from both the fixed charge distribution and the asymmetry in electron density over the ring system, making the phospholipid surface/interface the preferred localization of the NBD group in several membrane probes [37]. An extensive oligomerization of the antibiotic in the membrane would be expected to increase the measured energy transfer efficiencies due to the proximity of more than one acceptor due to the multimers formed, as it is schematically represented in Fig. 4C. This result would be translated to an apparent shorter tetraene-to-NBD separating distance, which was not found experimentally. Therefore, this hypothesis was ruled out and instead NBD-Nys is proposed to remain monomeric and anchored at the membrane surface (Fig. 4B).

4.2. Determination of the oligomeric state of the antibiotic in membranes by energy migration

In an attempt to further clarify the aggregation state of the polyene antibiotic Nys in lipid vesicles prepared with a variable lipid composition, polarized fluorescence measurements were carried for membrane-bound NBD-Nys. NBD fluorophore has a small Stokes shift (excitation peak 467 nm, emission peak 540 nm) contributing to its relatively large R_o value of ≈ 30 Å (Table 1). These distances are larger than the lateral dimensions of monomeric Nys, suggesting that efficient homotransfer could occur between subunits in a multimer [33]. A comparison of the theoretical concentration-dependent depolarization curves with the experimentally data provides a way of evaluating the association state of the antibiotic in the membranes. Fig. 3B shows

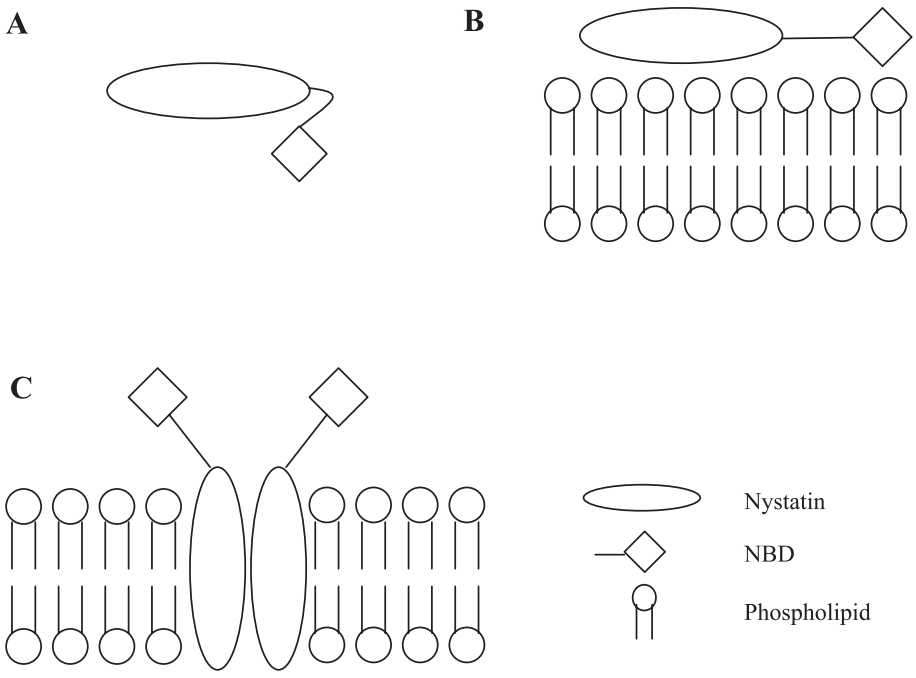

Fig. 4. Schematic representation of the putative conformations of NBD-Nys (A) in solution and (B,C) in the membranes. In (B), NBD-Nys is assumed to remain monomeric and anchored at the membrane surface whereas in (C), it has undergone oligomerization, which was accompanied by its translocation from the surface to the interior of the lipid bilayer.

that in none of the lipid mixtures used could a deviation from the expected behaviour for a random distribution of antibiotic labelled molecules in the surface of the membrane be detected. The absence of NBD fluorescence self-quenching (both dynamic and static) further supports the conclusion that there is no significant aggregation of the antibiotic derivative in the lipid vesicles. This result was intriguing, particularly for P10E LUV, because the fluorescence decays obtained for the antibiotic Nys confirmed independently its ability to oligomerize in these lipid vesicles within the same antibiotic concentration range (Table 2, $\lambda_{em}=410$ nm). Two different hypotheses can be put forward to explain these results. It can be speculated that NBD-Nys is assembling within the lipid vesicles but to a very small extent and the anisotropy measurements are not sensitive enough to detect this phenomenon, at variance with the time-resolved fluorescence measurements carried out with the parent compound, Nys. However, the simulations performed according to the monomer/dimer model of Loura and Prieto [19] show that, e.g., for $K_d=0.05$ mol/mol lipid and NBD-Nys: $L_{ac}=0.004$, approximately 12% of the antibiotic would be already engaged in dimer formation. In this case, $\langle r\rangle/\langle r\rangle_o$ would be expected to decrease from 0.863 to 0.821. Therefore, the steady-state anisotropy measurements should be able to report dimer formation. The use of higher surface concentrations of the NBD-labelled antibiotic could eventually help to clarify this question, because the more loaded the lipid vesicles are, the more probable is the formation of antibiotic aggregates. However, the addition of NBD-Nys to the lipid vesicles from a stock solution in methanol imposes some restrictions on the maximal volume of organic solvent that can be used without perturbing the membrane structure. It should also be mentioned that the dimerization model was used here to simulate the antibiotic aggregation in the membranes just for the sake of simplicity. In fact, higher-order aggregates are expected to be formed by Nys in the lipid vesicles [6,38], which should produce an even steeper decrease in the steady state fluorescence anisotropy of NBD-Nys than upon its dimerization [33].

Considering the previous discussion, we conclude that the chemical modification of Nys had a strong effect on its properties, influencing the antibiotic's ability to undergo aggregation in the lipid vesicles, probably due to stereochemical effects. Gary-Bobo and co-workers [39,40] has extensively studied the chemical properties of the polyene antibiotics that determine their selectivity towards cholesterol- and ergosterol-containing membranes. The authors found that AmB derivatives modified in its amino group were less efficient in permeabilizing the lipid vesicles, although their selectivity towards sterol-rich membranes remained almost unaltered. On the other hand, the simulation study carried out by Baginski et al. [41] also emphasized the importance of the charged groups in AmB mode of action, because the authors showed that the electrostatic interaction between the amine group of an antibiotic monomer and the carboxyl group of another was the main factor responsible for keeping the antibiotic channel open. We therefore conclude that (i) this NBD-hexanoyl derivative of Nys is not a good mimetic compound of Nys and accordingly studies using this probe (e.g., [42]) should be regarded

with caution and, (ii) the amine group of nystatin is an essential requisite for the supramolecular organization/pore formation of this antibiotic.

5. Conclusions

In this work, we studied the interaction of a NBD derivative of the polyene antibiotic nystatin with large unilamellar vesicles prepared with a variable sterol mole fraction. The membrane–water partition coefficients of NBD-Nys were of the same magnitude as the ones previously found for the nonderivatized antibiotic. The intrinsic chromophore (tetraene) of nystatin was used as a Förster pair with NBD to determine the mean interchromophoric distance of the lipid-bound antibiotic molecules ($R_o = 33$ Å in membranes). The distance measured ($R \approx 25$ Å) was larger than the one previously determined for the average conformation of the antibiotic in solution ($R \approx 18$ Å), implying that the antibiotic adopts a more extended conformation upon binding to cholesterol-containing membranes.

Energy migration (donor–donor energy transfer) is also an efficient process for the NBD chromophore ($R_o \approx 30$ Å) that was used here to evaluate the antibiotic aggregation state in the lipid vesicles. The fluorescence depolarization data obtained was well described by a model that assumes a random distribution of molecules which suggests a nonsignificant aggregation of the derivatized species. Altogether, our data suggests that this NBD derivative does not report adequately the nystatin channel-forming properties or dynamics, at variance with the study of O'Neill et al. [42].

Acknowledgements

The authors are grateful to Luís Loura for discussion and suggestions. This study was supported by project POCTI/36389/FCB/2000 (Fundação para a Ciência e Tecnologia, Portugal).

Appendix A. Determination of energy transfer efficiencies for membrane-bound NBD-Nys

The overall fluorescence emitted by an antibiotic sample in the presence of lipid vesicles, I^j (j = Nys or NBD-Nys) depends on the contributions of all species:

$$I^j = \sum_i x_i^j I_i^j \tag{A1}$$

where x_i^j and I_i^j are the fractional population and the fluorescence intensity of each species (i = w or m for aqueous and membrane-bound molecules, respectively).

The overall efficiency of energy transfer, E, between the tetraene and the NBD chromophores for NBD-Nys in the presence of lipid vesicles, calculated according to Eq. (8), is therefore:

$$E = 1 - \frac{x_w^{\mathrm{NBD-Nys}} I_w^{\mathrm{NBD-Nys}} + x_m^{\mathrm{NBD-Nys}} I_m^{\mathrm{NBD-Nys}}}{x_w^{\mathrm{Nys}} I_w^{\mathrm{Nys}} + x_w^{\mathrm{Nys}} I_w^{\mathrm{Nys}}} \tag{A2}$$

In the limiting cases, i.e., considering that either all the molecules remain in the aqueous solution or are membrane-bound, Eq. (A2) reduces to:

$$E_i = 1 - \frac{I_i^{\mathrm{NBD-Nys}}}{I_i^{\mathrm{Nys}}} \tag{A3}$$

Using these definitions, Eq. (A2) can be rewritten as:

$$E_m = \frac{(x_w^{\mathrm{NBD-Nys}} + x_w^{\mathrm{Nys}} \cdot E - x_w^{\mathrm{Nys}}) I_w^{\mathrm{Nys}} + (x_m^{\mathrm{NBD-Nys}} + x_m^{\mathrm{Nys}} \cdot E - x_m^{\mathrm{Nys}}) I_m^{\mathrm{Nys}}}{x_m^{\mathrm{NBD-Nys}} \cdot I_m^{\mathrm{Nys}}} \tag{A4}$$

If $K_p^{\mathrm{Nys}} \approx K_p^{\mathrm{NBD-Nys}}$, then $x_i^{\mathrm{Nys}} \approx x_i^{\mathrm{NBD\text{-}Nys}}$, and, hence:

$$E_m = E\left(1 + \frac{I_w^{\mathrm{Nys}}}{I_m^{\mathrm{Nys}}}\right) \tag{A5}$$

Because $\Phi_m^{\mathrm{Nys}} \gg \Phi_w^{\mathrm{Nys}}$, the ratio $I_w^{\mathrm{Nys}}/I_m^{\mathrm{Nys}}$ is very small, and under these conditions Eq. (A5) becomes $E \approx E_m$. Therefore, it is possible to conclude that although the aqueous antibiotic mole fractions were relatively high in all the systems studied (≈ 70–75%), the efficiency of energy transfer measured for NBD-Nys in the presence of the lipid vesicles were largely dominated by the fractional contribution from the antibiotic molecules partitioned into the membranes.

References

[1] J. Bolard, How do the polyene macrolide antibiotics affect the cellular membrane properties? Biochim. Biophys. Acta 864 (1986) 257–304.
[2] N. Akaike, N. Harata, Nystatin perforated patch recording and its applications to analyses of intracellular mechanisms, Jpn. J. Physiol. 44 (1994) 433–473.
[3] W.I. Gruszecki, M. Gagos, P. Kernen, Polyene antibiotic amphotericin B in monomolecular layers: spectrophotometric and scanning force microscopic analysis, FEBS Lett. 524 (2002) 92–96.
[4] S.C. Hartsel, C. Hatch, W. Ayenew, How does amphotericin B work? Studies on model membrane systems, J. Liposome Res. 3 (1993) 377–408.
[5] R.A. Brutyan, P. McPhie, On the one-sided action of amphotericin B on lipid bilayer membranes, J. Gen. Physiol. 107 (1996) 69–78.
[6] G. Fujii, J.-E. Chang, T. Coley, B. Steere, The formation of amphotericin B ion channels in lipid bilayers, Biochemistry 36 (1997) 4959–4968.
[7] B.E. Cohen, Amphotericin B toxicity and lethality: a tale of two channels, Int. J. Pharm. 162 (1998) 95–106.
[8] B.E. Cohen, A sequential mechanism for the formation of aqueous channels by amphotericin B in liposomes. The effect of sterols and phospholipid composition, Biochim. Biophys. Acta 1108 (1992) 49–58.
[9] J. Bolard, P. Legrand, F. Heitz, B. Cybulska, One-sided action of

amphotericin B on cholesterol-containing membranes is determined by its self-association in the medium, Biochemistry 30 (1991) 5707–5715.
[10] B.V. Cotero, S. Rebolledo-Antúnez, I. Ortega-Blake, On the role of sterol in the formation of the amphotericin B channel, Biochim. Biophys. Acta 1375 (1998) 43–51.
[11] B.D. Wolf, S.C. Hartsel, Osmotic stress sensitizes sterol-free phospholipid bilayers to the action of amphotericin B, Biochim. Biophys. Acta 1238 (1995) 156–162.
[12] T. Ruckwardt, A. Scott, J. Scott, P. Mikulecky, S.C. Hartsel, Lipid and stress dependence of amphotericin B ion selective channels in sterol-free membranes, Biochim. Biophys. Acta 1372 (1998) 283–288.
[13] A. Coutinho, M. Prieto, Self-association of the polyene antibiotic nystatin in dipalmitoylphosphatidylcholine vesicles. A time-resolved fluorescence study, Biophys. J. 69 (1995) 2541–2557.
[14] A. Coutinho, M. Prieto, Cooperative partition model of nystatin interaction with phospholipid vesicles, Biophys. J. 84 (5) (2003) 3061–3078.
[15] A. Coutinho, M. Prieto, Interaction between nystatin and phospholipid vesicles: the sterol dependence, Prog. Biophys. Mol. Biol. 120 (1996) 120.
[16] N.O. Petersen, Intramolecular fluorescence energy transfer in nitrobenzoxadiazole derivatives of polyene antibiotics, Can. J. Chem. 63 (1985) 77–85.
[17] L. Silva, A. Coutinho, A. Fedorov, M. Prieto, Solution conformation of a nitrobenzoxadiazole derivative of the polyene antibiotic nystatin: a FRET study, J. Photochem. Photobiol., B (2003) (in press).
[18] B. Snyder, E. Freire, Fluorescence energy transfer in two dimensions: a numeric solution for random and non-random distributions, Biophys. J. 40 (1982) 137–148.
[19] L.M.S. Loura, M. Prieto, Dehydroergosterol structural organization in aqueous medium and in a model system of membranes, Biophys. J. 72 (1997) 2226–2236.
[20] L.D. Mayer, M.J. Hope, P.R. Cullis, Vesicles of variable sizes produced by a rapid extrusion procedure, Biochim. Biophys. Acta 858 (1986) 161–168.
[21] C. McClare, An accurate and convenient organic phosphorus assay, Anal. Biochem. 39 (1971) 527–530.
[22] S.H. White, W.C. Wimley, A.S. Ladokhin, K. Hristova, Protein folding in membranes: determining energetics of peptide-bilayer interactions, Methods Enzymol. 295 (1998) 62–87.
[23] S.R. Meech, D. Phillips, Photophysics of some common fluorescence standards, J. Photochem. 23 (1983) 193–217.
[24] S.F. Fery-Forgues, J.P. Fayet, A. Lopez, Drastic changes in the fluorescence properties of NBD probes with the polarity of the medium: involvement of a TICT state? J. Photochem. Photobiol., A: Chem. 70 (1993) 229–243.
[25] J.R. Lakowicz, Principles of Fluorescence Spectroscopy, 2nd edn., Plenum, New York, 1999.
[26] L.M.S. Loura, A. Fedorov, M. Prieto, Partition of membrane probes in a gel/fluid two-component lipid system: a fluorescence resonance energy transfer study, Biochim. Biophys. Acta 1467 (1) (2000) 101–112.
[27] A. Coutinho, J. Costa, J.L. Faria, M.N. Berberan-Santos, M. Prieto, Dibucaine interaction with phospholipid vesicles. A resonance energy transfer study, Eur. J. Biochem. 189 (1990) 387–393.
[28] J. Eisenberg, W.E. Blumberg, R.E. Dale, Orientational effect in intra- and intermolecular long range excitation energy transfer, Ann. N. Y. Acad. Sci. 366 (1981) 155–175.
[29] A. Chattopadhyay, E. London, Spectroscopic and ionization properties of *N*-(7-nitrobenz-2-oxa-1,3-diazol 4 yl)-labelled lipids in model membranes, Biochim. Biophys. Acta 938 (1988) 24–34.
[30] S. Mazères, V. Schram, J.F. Tocanne, A. Lopez, 7-Nitrobenz-2-oxa-1,3-diazole-4-yl-labelled phospholipids in lipid membranes: differences in fluorescence behaviour, Biophys. J. 71 (1996) 327–335.
[31] L. Lupan, R. Bandula, M. Vasilescu, C. Bercu, Spectroscopy study on nystatin conformational modifications generated by its interaction with the solvent, Fresenius' J. Anal. Chem. 355 (1996) 409–411.
[32] M.J. Prieto, M. Castanho, A. Coutinho, A. Ortiz, F.J. Aranda, J.C. Gomez-Fernandez, Fluorescence study of a derivatized diacylglycerol incorporated in model membranes, Chem. Phys. Lipids 69 (1994) 75–85.
[33] L.W. Runnels, S.F. Scarlata, Theory and application of fluorescence homotransfer to melittin oligomerization, Biophys. J. 69 (1995) 1569–1583.
[34] S.M. Blackman, D.W. Piston, A.H. Beth, Oligomeric state of human erythrocyte band 3 measured by fluorescence resonance energy homotransfer, Biophys. J. 75 (1998) 1117–1130.
[35] J.M. Smaby, M.M. Monsen, H.L. Brockman, R.E. Brown, Phosphatidylcholine acyl unsaturation modulates the decrease in interfacial elasticity induced by cholesterol, Biophys. J. 73 (1997) 1492–1505.
[36] S. Mukherjee, A. Chattopadhyay, A. Samanta, T. Soujanya, Dipole moment change of NBD group upon excitation studied using solvatochromic and quantum chemical approaches: implications in membrane research, J. Phys. Chem. 98 (1994) 2809–2812.
[37] D. Huster, P. Müller, K. Arnold, A. Herrmann, Dynamics of membrane penetration of the fluorescent 7-nitrobenz-2-oxa-1,3-diazol-4-yl (NBD) group attached to an acyl chain of phosphatidylcholine, Biophys. J. 80 (2001) 822–831.
[38] M.E. Kleinberg, A. Finkelstein, Single-length and double-length channels formed by nystatin in lipid bilayer membranes, J. Membr. Biol. 80 (1984) 257–269.
[39] C.M. Gary-Bobo, Polyene–sterol interaction and selective toxicity, Biochimie 71 (1989) 37–47.
[40] M. Hervé, J.C. Debouzy, E. Borowski, B. Cybulska, C. Gary-Bobo, The role of the carboxyl and amino groups of polyene macrolides in their interactions with sterols and their selective toxicity. A ^{31}P-NMR study, Biochim. Biophys. Acta 980 (1989) 261–272.
[41] M. Baginski, H. Resat, J.A. McCammon, Molecular properties of amphotericin B membrane channel: a molecular dynamics simulation, Mol. Pharmacol. 52 (1997) 560–570.
[42] L.J. O'Neill, J.G. Miller, N.O. Petersen, Evidence for nystatin micelles in L-cell membranes from fluorescence photobleaching measurements of diffusion, Biochemistry 25 (1986) 177–181.